

The Influence of Selected Technological Parameters on Changes in the Flanging Load

Tomasz Miłek^{1*}

¹ Faculty of Mechatronics and Mechanical Engineering, Kielce University of Technology, Al. Tysiąclecia Państwa Polskiego 7, 25-314 Kielce, Poland

* Corresponding author's e-mail: tmاتم@tu.kielce.pl

ABSTRACT

The flanging process is widely used in stamping production: when collar drawing small holes for threads or to increase the stiffness of a draw piece. It can also replace the operation of deep drawing cylindrical draw pieces with a large flange followed by cutting the bottom. The paper discusses the influence of the shape of the punch and the grade of material on load changes at various collar drawing coefficients. Flat, spherical and conical punches and samples made of EN-AW 1050A aluminium, Cu-ETP copper, CuZn37 brass, S235JRG2 steel, X6Cr17 steel and X5CrNi18-10 steel were used for testing. The relative thickness of test pieces was 0.015 (which corresponded to a thickness of 1 mm and a blank diameter of 66 mm). Various collar drawing factors ranging from 0.32 to 0.54 were adopted in the studies. An analysis of the obtained height of collars and wall thicknesses was carried out. The experimental tests were carried out using special tooling mounted on a testing machine with a 20 kN load for 0.5 metrological class. Changes in the force as a function of the displacement of the punches were recorded using Test&Motion software that is commonly applied in research laboratories. Based on the obtained results at various technological parameters, possibility of flanging process was evaluated in industrial conditions.

Keywords: flanging, collar drawing, flanging load, changes in flanging load, technological parameters of flanging, collar drawing coefficient

INTRODUCTION

Flanging the edges of holes involves forming a relatively low edge around a hole of appropriate diameter or other dimensions previously cut in the blank or in the draw piece (for flanging the edges of non-round holes) [1]. Collar drawing is widely used in stamping production: when flanging small holes for threads, pressing an axle into a flared rim or to increase the stiffness of a draw piece [2, 3]. Flanges are used to improve appearance, stiffness, hidden joints and reinforce the edges of sheet metal parts [4]. It can also replace the operation of deep drawing cylindrical draw piece with a large flange followed by cutting the bottom [5].

In flanging process, the material elongates in the tangential direction and the material thickness decreases. The most common phenomenon that limits the collar drawing around holes is radial

cracking of the material at the edge of the hole and longitudinal cracks running along the forming side surface of the flange or, less commonly, circumferential cracking of the material near the edge of the die [6]. The degree of deformation at flanging process is determined by the ratio of the diameter of the hole in the semi-finished product to the diameter of the flange, i.e. the so-called flanging (collar drawing) coefficient [1–6]:

$$k_w = \frac{d}{D} \quad (1)$$

where: d – diameter of the hole before flanging, mm; D – diameter of flanging (in middle of thickness), mm.

The value of the collar drawing factor depends on [1–3]:

1. Method of making the hole. Slightly higher coefficients are obtained in the case of holes

after blanking before flanging process than in the case of drilled holes.

2. The relative thickness of the blank ratio (g_0/D_0 , where: g_0 – initial thickness of the blank, D_0 – diameter of the blank). As the relative thickness of the blank increases, the value of the permissible collar drawing coefficient decreases.
3. Type of material and its mechanical properties.
4. The shape of the working part of the punch.

Flanging is still a very important sheet forming method used in the engineering industry. Recent investigations shows the use of so-called modern materials for collar drawing process, such as AHSS type high strength steels, manganese-boron steels (22MnB5), TWIP steels with a high content of manganese, light alloys (mainly magnesium as well as high strength aluminium from the 7xxx group) [7]. Over the last 25 years, many authors have conducted research on the influence of punch shape on selected parameters of the curling process. The most common shapes of the working part were conical, cylindrical and spherical or semi-spherical at various dimensions. The following brief review of research results applies only to selected works [4, 5, 8–14].

Leu et al. [8] used FEM to predict the flange extension limit conditions until unloading for three typical punch shapes with experimental verification. Chalupczak et al. [5], based on the obtained experimental results of flanging with various punches and types of materials (mainly non-ferrous metals and their alloys), verified the available relationships from the literature used to calculate the technological parameters of the process (values of forces, wall thickness and rim height). Huang et al. [9] examined the influence of the cone semi-angle of various conical punches on the limitation of formability in the flanging process. They used low-carbon sheet plate with a thickness of 1.18 mm in their investigations. In his other work, Huang [10] stated that reducing the punch diameter and increasing the flange height significantly reduced the flange thickness (tests for the same steel grade). Stachowicz [4] determined impact the punch geometry (cylindrical, hemispherical and conical) and mechanical properties parameters (especially strain hardening and plastic anisotropy) on the limit expansion of the hole. He conducted a series of investigations into flanging with three different kinds of 1.0 mm thick steel sheet: DQ drawing quality, DDQ deep drawing quality and EDQ extra drawing quality. In other paper Frącz and Stachowicz [11]

discussed the sheet thickness distribution along collar after hole-flanging of the same grade of steel sheet. They demonstrated that the reduction of the sheet thickness depends on a forming punch shape and observed the largest sheet thickening for collars formed with cylindrical (flat bottomed) punch. Krawczyk et al. [12] conducted tests on the flanging of samples in which holes were cut using various technologies: laser cutting, electro-discharge method using wire and punching. Their investigations have revealed that the shape of the used tools has a great impact on the final diameter of the hole after flanging. The greatest enlargement of the diameter they obtained for the conical punch and the smallest expansion for the cylindrical punch. Kumar et al. [13] conducted investigations for six punches i.e. cylindrical, two stepped, three stepped, six stepped, conical and hemispherical geometry. They demonstrated that circumferential and radial strain and load requirement to form the flange are minimum in hemispherical punch profile as compared to other punch shapes

Another group of authors develops the concept of incremental forming in their research on flanging [14, 15]. Wang et al. [14] designed the multi-step flanging in one press stroke accomplished by a novel punch with a notch. Bambach et al. [15] in their work proposed two new approaches in incremental forming: an adaptive blank holder and new process set-up that makes it possible to perform flanging operations at high speed. Sousse et al. [16] investigated impact of the initial hole diameter on the state of the flange taking consideration a such defects as necking and tearing of rims and thickness of crack initiation. In their other paper [17], the flanged hole is adopted as a potential solution to increase the number of formed threads for sheet metal part. Balawender et al. [18] presented the results of research on shaping the edges of flange holes made of titanium alloys at elevated temperatures by friction heating of the flange area.

The research included in the paper determined the possibilities and limits of the collar drawing coefficients, the maximum values of the flanging forces, the heights and minimum wall thicknesses of the flanged edge, and the changes in the forces for different materials and shapes of the working parts of the punches. The test materials, i.e. aluminium, copper, brass and three grades of steel, were selected for their various applications and mechanical properties. The specific aim of the research in the paper was to determine the impact of selected technological parameters, such as the

shape of the working part of the punch (flat, conical and spherical) and the diameter of the drilled hole ($d = 10\text{ mm}$, 7.5 mm , 6 mm , which corresponded to different degrees of deformation) on changes in the flanging force for various materials.

METHODOLOGY

Six types of materials with different mechanical properties, made of sheet metal with nominal thicknesses of $g_0 = 1\text{ mm}$, were used for experimental tests of the collar drawing process. These were EN-AW 1050A aluminium ($g_0 = 0.970\text{ mm}$), Cu-ETP copper ($g_0 = 0.997\text{ mm}$), CuZn37 brass ($g_0 = 0.995\text{ mm}$), S235JRG2 steel ($g_0 = 0.970\text{ mm}$), X6Cr17 steel ($g_0 = 0.998\text{ mm}$) and X5CrNi18-10 steel ($g_0 = 0.985\text{ mm}$), respectively. The average thickness values from five measurements made using a micrometer screw are given in brackets. When selecting materials for testing, their wide applications in various industries (manufacture of elements with specific operational requirements) were taken into account.

Mechanical properties were determined based on a static tensile test [19]. It was carried out on a LabTest 5.20SP1 testing machine with a 20 kN load for 0.5 metrological class. For this purpose, samples with dimensions consistent with the standard [19] were prepared, as shown in Figure 1.

The determined mechanical properties of the tested materials (average values from three samples) are presented in Table 1. On their basis, it was found that EN-AW 1050A aluminium and Cu-ETP copper have the characteristics of materials strengthened by rolling. However, the properties of CuZn37 brass and three types of steel (S235JRG2, X6Cr17 and X5CrNi18-10) are similar to those of materials in the as-annealed condition. The graphs obtained in the tensile test (force vs. displacement), processed in the GRAPHER software, are shown in Figure 2. The determined relationships between relative strain and flow stress for individual materials are shown in Figure 3.

The relative strain ε was calculated from the formula (2) [2, 3]:

$$\varepsilon = \frac{\Delta L}{L_0} \tag{2}$$

where: ΔL – displacement, mm; L_0 – initial length of the measuring part of the test piece, mm.

The flow stress σ_p was calculated from formula (3) [2, 3]:

$$\sigma_p = \frac{F}{S_0} \tag{3}$$

where: F – force, N; S_0 – initial test piece cross-section, mm^2 .

Samples for flanging tests were prepared in the form of blanks with a $D_0 = 66\text{ mm}$, punched on an

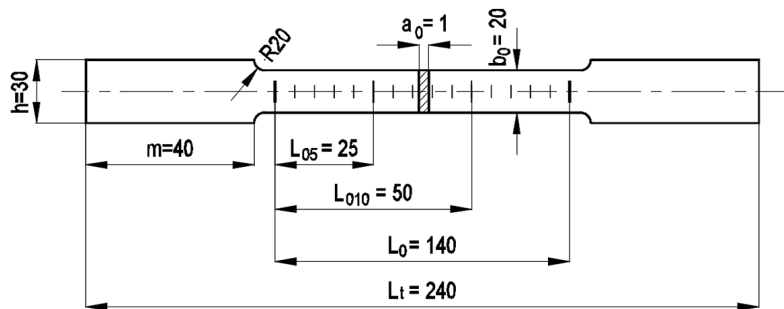


Figure 1. Dimensions of the flat test pieces used in the experiment

Table 1. Mechanical properties of test pieces used in the investigations

Material	R_m (MPa)	$R_{p0.2}$ (MPa)	A (%)	$A_{11.3}$ (%)
EN-AW 1050A aluminium	121.9	117	16	12
Cu-ETP copper	253.2	209	41	33
CuZn37 brass	364.3	235	54	45
S235JRG2 steel	290.3	142	61	50
X5CrNi18-10 steel	710.9	314	62	54
X6Cr17 steel	456.6	298	46	37

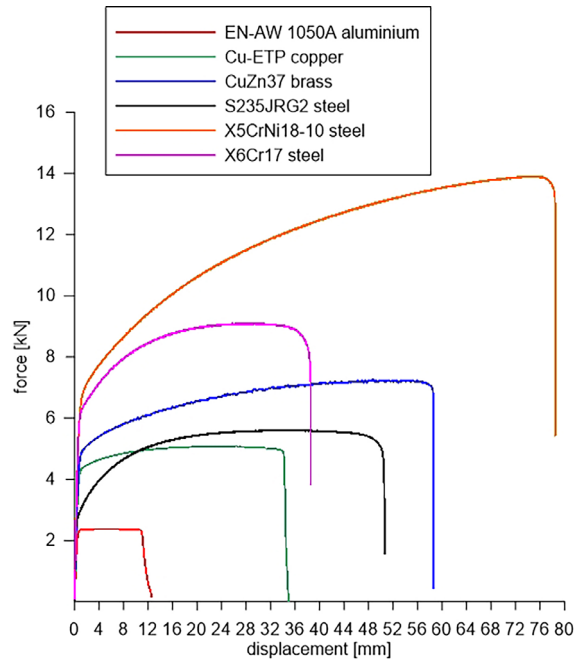


Figure 2. The force vs. displacement obtained for static tensile test for test pieces made from different materials

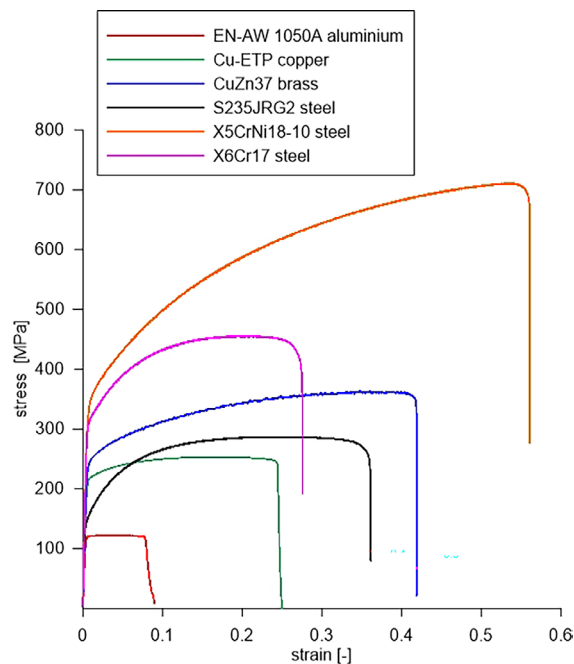


Figure 3. The stress vs. relative strain obtained for static tensile test for test pieces made from different materials

industrial blanking tool mounted on a BUSSMAN hydraulic press with a maximum load of 1 MN (which corresponded to a relative material thickness $g_0/D_0 = 0.015$). Holes of different diameters $d = 10$ mm, 7.5 mm and 6 mm were drilled in them. Laboratory press tool was used for flanging, the main elements of which are shown and

described in Figure 4. View of this tooling is presented in Figure 5. A blank holder was used in the course of the collar drawing (Fig. 4 and Fig. 5) because the literature-based condition of $g_0/D_0 \leq 0.02$ was satisfied [1]. It prevented the formation of folds and cracks in the material. Laboratory tooling was installed on the LabTest5.20SP1

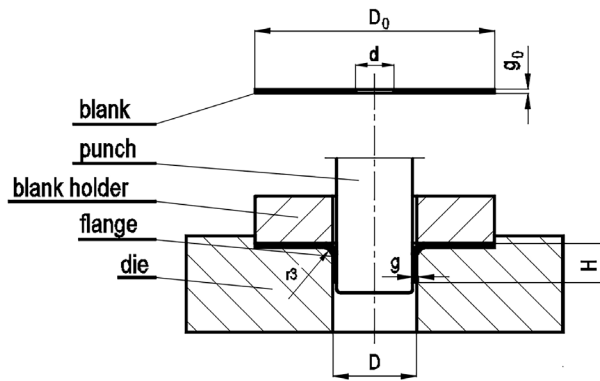


Figure 4. Schematic representation of flanging process

testing machine and, for X5CrNi18-10 steel samples, on the ZD100 press (for 1 metrological class) with a maximum load of 1MN, because their flanging force exceeded 20 kN. Different stamp shapes and their dimensions used in the research are shown in Figure 6. The diameter of the punches was 17.5 mm and the die diameter was 20 mm. All obtained results in terms of forces and

displacements of the punch were recorded using specialized Test&Motion software used in industrial research laboratories.

The adopted dimensions and shapes of the stamps result from the analysis of guidelines contained in the literature [2, 3], initially verified in pilot studies for certain materials [5].

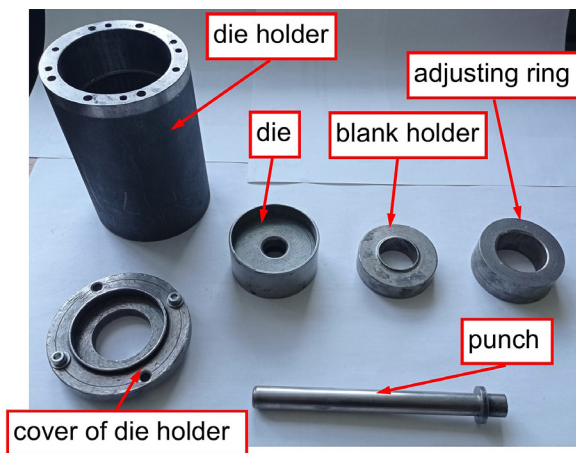


Figure 5. View of tooling used in experiment of flanging process

RESULTS AND ANALYSIS

The obtained test results showed that it is possible to flange the edges of holes without cracks and tears for all collar drawing coefficients and the three punch shapes used, in the case of flanging of S235JRG2 steel. Similar results were obtained for X5CrNi18-10 steel samples, except for test pieces flanged with a spherical punch at the coefficient $k_3 = 0.32$ (for which a longitudinal cracks running along the forming side surface of the flange of approximately 3 mm long appeared). When flanging samples from EN-AW 1050A aluminium, Cu-ETP copper, CuZn37 brass and X6Cr17 steel for drilled hole diameters $d = 10$ mm (which

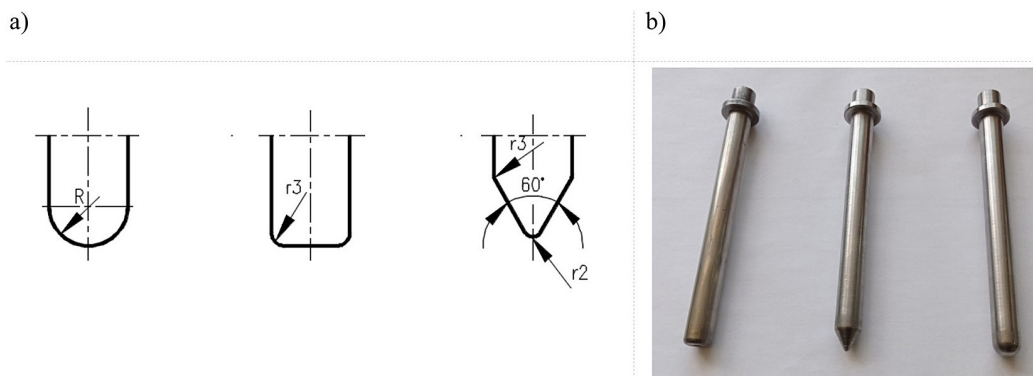


Figure 6. Punches used in experiment: a) shape and dimensions, b) view

corresponded to the collar drawing coefficient $k_1 = 0.54$), regardless of the shape of the punches, the flanged edges had no defects. Exemplary samples made from these materials are shown in Figure 7. The flanging was successful for all punch shapes and the coefficient $k_2 = 0.41$ only for H17 steel samples. However, reducing the coefficient to $k_3 = 0.32$ for these samples in each case caused longitudinal cracks of the material. The flanging of the hole $d = 7.5$ mm ($k_2 = 0.41$ respectively) was also successfully completed with a flat and conical punch for samples made from Cu-ETP copper and CuZn37 brass. With a spherical punch and factor $k_2 = 0.41$ (single cracks about 1 mm long) and with all punch shapes and factor $k_3 = 0.32$, copper and brass samples cracked on the periphery of the flanged hole. Tests to make the edges of holes from EN-AW 1050A aluminium for $k_2 = 0.41$ with flat and conical punches and in each case at $k_3 = 0.32$ ended in failure, because already in the initial phases of flanging,

the material cracked similarly to copper, brass and steel samples. Folding of the tested materials with larger hole diameters than $d = 10$ mm was not carried out because the height of the rim in this case would be very small and their usefulness in production conditions was negligible.

Table 2 shows the values of the maximum forces F obtained when flanging the edges of holes for various materials and punch shapes (average results from three measurements).

They depend on the shape of the punch. With the same coefficient in each case, the highest values occur with a flat punch. For the collar drawing coefficients $k_1 = 0.54$ and $k_2 = 0.41$, the highest flanging forces were obtained for flat punches, then smaller ones respectively for conical and spherical punches (except for the brass sample for which, with the coefficient $k_2 = 0.41$, the flanging force of the spherical punch was greater than the flanging force of the conical punch, but only by approximately 1.2%). With the coefficient $k_3 = 0.32$, the

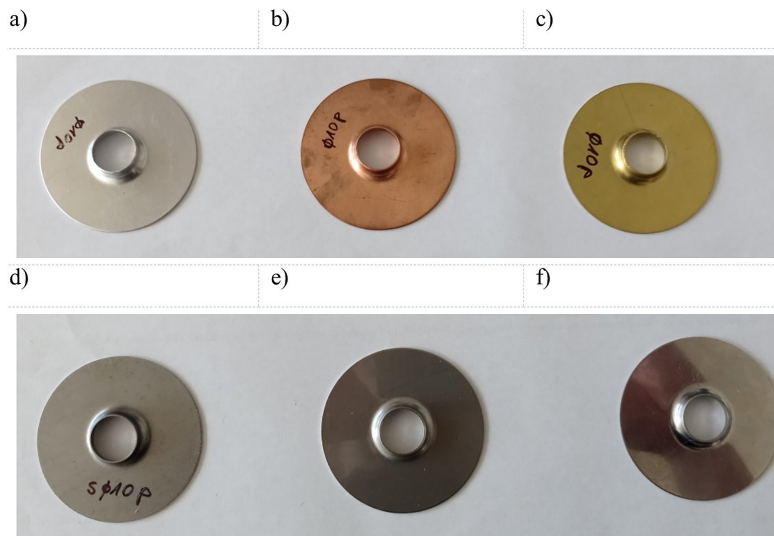


Figure 7. Samples after flanging at the same coefficient $k_1 = 0.54$ made from: a) EN-AW 1050A aluminium, b) Cu-ETP copper, c) CuZn37 brass, d) S235JRG2 steel, e) X5CrNi18-10 steel, f) X6Cr17 steel

Table 2. The maximum values of flanging forces (N) obtained in investigations

k_n	Shape of punch	EN-AW 1050A	Cu-ETP	CuZn37	S235JRG2	X5CrNi18-10	X6Cr17
0.54	flat	2024.32	4194.78	5597.54	5772.62	10141.78	8698.06
	conical	1747.44	3686.32	4893.86	4766.88	8504.66	6871.76
	spherical	1573.48	3263.32	4349.60	4291.42	7560.32	6190.44
0.41	flat	2612.20	5691.06	8044.72	8396.58	15779.58	11682.26
	conical	2024.88	4409.58	5988.64	6064.60	11912.72	8622.56
	spherical	1989.78	4274.08	6061.80	5886.16	11400.90	8415.58
0.32	flat	3078.16	6700.72	10335.32	10385.10	20410.83	14171.96
	conical	1795.54	4665.64	6898.04	6401.32	13545.48	9266.94
	spherical	2097.18	4920.70	7241.50	7087.66	14229.02	9943.76

highest forces were also obtained for flat punches, but smaller forces were obtained for spherical and conical punches (i.e. a different order than for the coefficients $k_1 = 0.54$ and $k_2 = 0.41$). For the coefficient $k_1 = 0.54$, the use of conical punches resulted in a reduction in the flanging force compared to flat punches by 12–13.7% for non-ferrous metals and their alloys (aluminium, copper and brass) and by 16–21% for steel samples. However, the use of spherical punches at this coefficient resulted in a reduction in the flanging force compared to flat punches by approximately 22% for non-ferrous metals and their alloys and by 26–29% for steel samples. Reducing the coefficients from $k_1 = 0.54$ to $k_2 = 0.41$ and then $k_3 = 0.32$ resulted in increased differences between the forces.

At the coefficient $k_2 = 0.41$, the use of conical punches resulted in a reduction in the flanging force compared to flat punches by 23–26% for non-ferrous metals and their alloys and by 25–28% for steel samples. However, the use of spherical punches resulted in a reduction in the flanging force compared to flat punches by approximately 24–25% for non-ferrous metals and their alloys and by 28–30% for steel samples. With the coefficient $k_3 = 0.32$, the use of spherical punches resulted in a reduction in the flanging force compared to flat punches by 27–32% for non-ferrous metals and their alloys and by 30–32% for steel samples. However, the use of conical punches resulted in a reduction in the flanging force compared to flat punches by approximately 31–42% for non-ferrous metals and their alloys and by 34–38% for steel samples.

Based on the above analysis, it was found that at the limit degrees of deformation (i.e. the lowest

collar drawing coefficients) for the materials examined in the paper, the lowest flanging forces occur for conical punches, and not, as the authors of note in their works [13], for spherical punches. The lowest flanging forces are recorded for spherical punches, but with higher collar drawing coefficients than the limit ones.

In the next stage of the experimental investigations, changes in flanging forces as a function of punch displacement were analysed for individual materials with different punches and the same collar drawing coefficients. They are presented in Figures 8–13.

Changes in forces as a function of punch displacement are similar in nature regardless of the punch shapes adopted, the coefficients of collar drawing and the type of material. For the same factors, the graphs differ in the total displacement values of the punch at flanging, the maximum force values and the displacement values at which these maximum forces occur. The smallest total displacements are found with flat punches, regardless of the type of material. Flanging with a spherical punch increases the displacement by approximately 18–40% for $k_1 = 0.54$, 25–36% for $k_2 = 0.41$ and 15–31% for $k_3 = 0.32$, respectively. However, flanging with a conical punch increases the displacement compared to flanging with a flat punch by approximately 40–50% for $k_1 = 0.54$, 50–63% for $k_2 = 0.41$ and 33–54% for $k_3 = 0.32$.

When flanging the edges of holes with a flat punch (Figures 8–13), the force increases rapidly when the process starts and reaches its maximum value with a relatively small displacement distance of the punch. When using a spherical punch for flanging, the maximum value of force is achieved

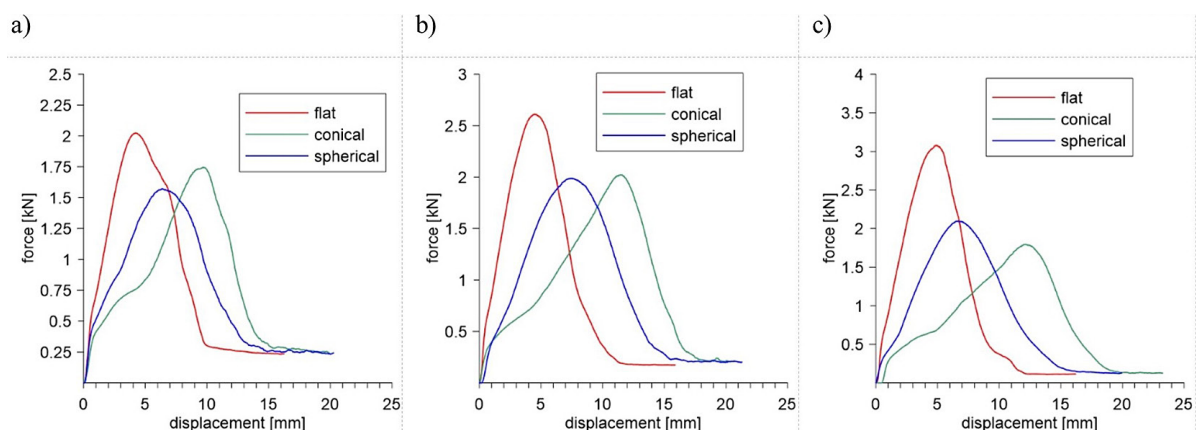


Figure 8. The force vs. displacement obtained for flanging tests from samples made from EN-AW 1050A aluminium with different shape of punch (flat, conical and spherical) and various collar drawing factors (k): a) at $k_1 = 0.54$; b) at $k_2 = 0.41$; c) at $k_3 = 0.32$

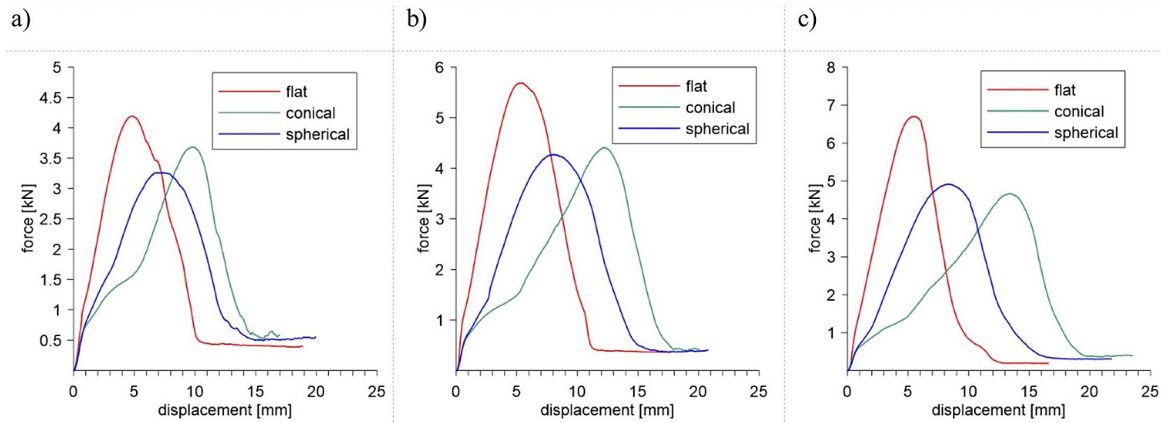


Figure 9. The force vs. displacement obtained for flanging tests from samples made from Cu-ETP copper with different shape of punch (flat, conical and spherical) and various collar drawing factors (k): a) at $k_1 = 0.54$; b) at $k_2 = 0.41$; c) at $k_3 = 0.32$

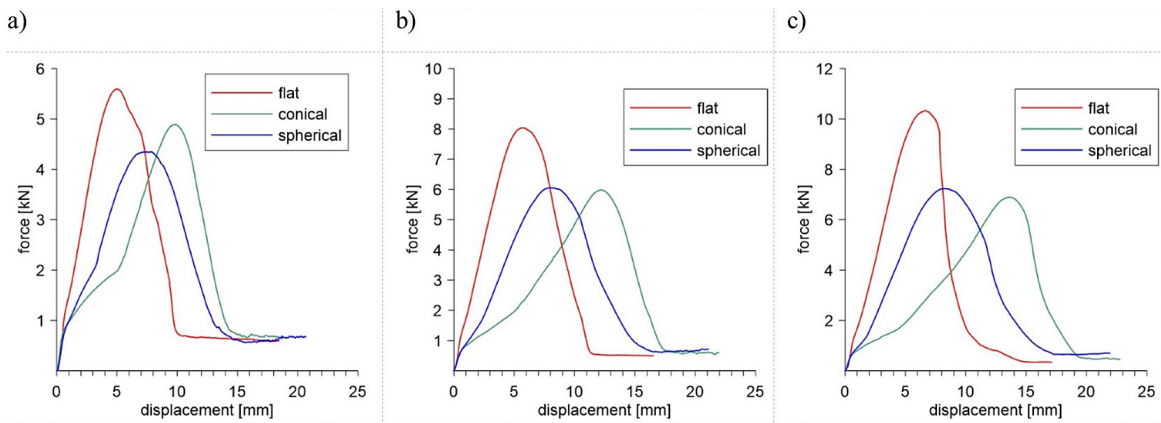


Figure 10. The force vs. displacement obtained for flanging tests from samples made from CuZn37 brass with different shape of punch (flat, conical and spherical) and various collar drawing factors (k): a) at $k_1 = 0.54$; b) at $k_2 = 0.41$; c) at $k_3 = 0.32$

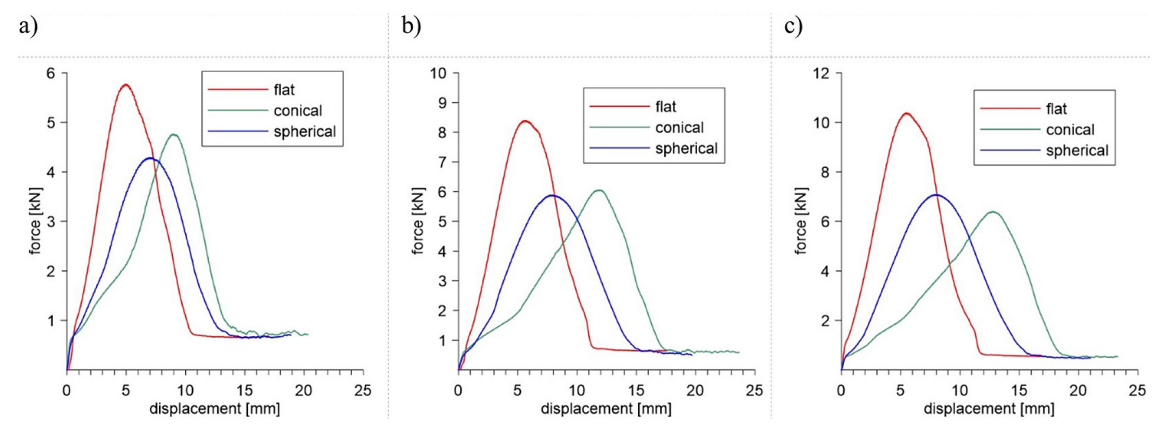


Figure 11. The force vs. displacement obtained for flanging tests from samples made from S235JRG2 steel with different shape of punch (flat, conical and spherical) and various collar drawing factors (k): a) at $k_1 = 0.54$; b) at $k_2 = 0.41$; c) at $k_3 = 0.32$

with a larger displacement of the punch compared to the displacement with a flat punch (by about 75%), and to obtain the maximum force when

flanging with a conical punch, an even greater displacement of the punch is needed (by about 125%). With an increase in the degree of deformation

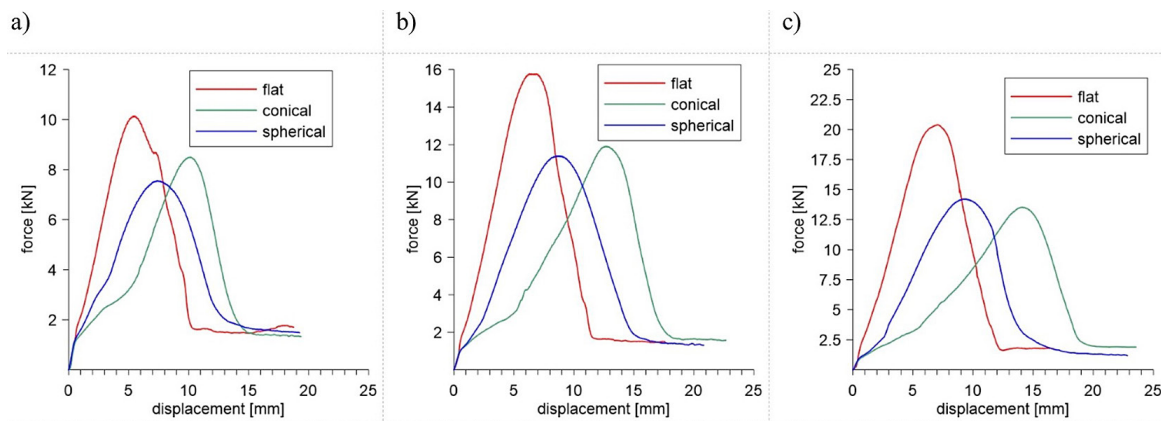


Figure 12. The force vs. displacement obtained for flanging tests from samples made from X5CrNi18-10 steel with different shape of punch (flat, conical and spherical) and various collar drawing factors (k): a) at $k_1 = 0.54$; b) at $k_2 = 0.41$; c) at $k_3 = 0.32$

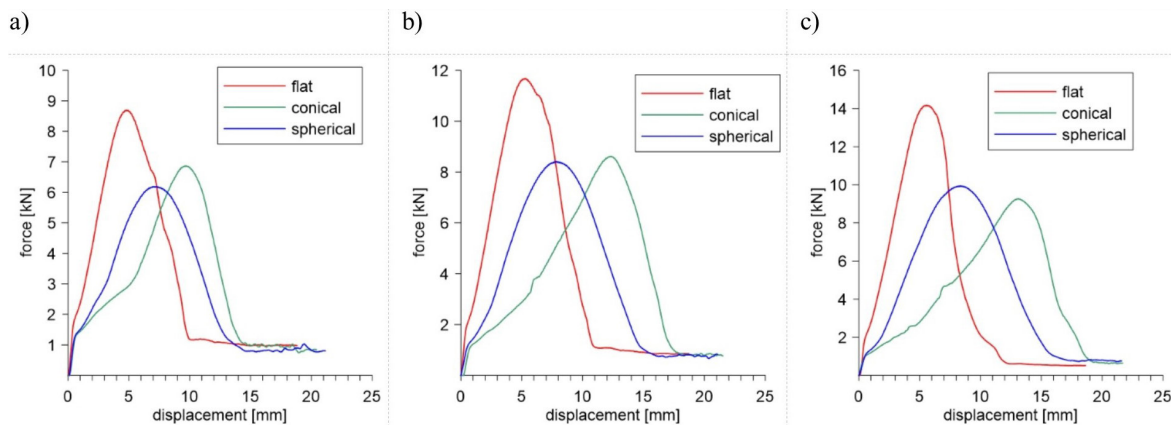


Figure 13. The force vs. displacement obtained for flanging tests from samples made from X6Cr17 steel with different shape of punch (flat, conical and spherical) and various collar drawing factors (k): a) at $k_1 = 0.54$; b) at $k_2 = 0.41$; c) at $k_3 = 0.32$

(i.e. a decrease in the collar drawing coefficient), the displacement at which the maximum value of force occurs when flanging with a conical punch increases significantly (an increase of about 45% for $k_3 = 0.32$ compared to $k = 0.54$). For other punch shapes (flat and spherical), these differences are smaller and amount to 25–30%.

The cumulative graphs in Figures 14–16 summarise the variation of the flanging forces shown earlier (Figures 8–13) as a function of punch displacement for different materials.

In the group of non-ferrous metals and their alloys, with the same collar drawing coefficients, the highest force values were obtained for brass and the lowest for aluminium. The increase in the force values for brass compared to aluminium was approximately 176–284% depending on the collar drawing coefficient (respectively for $k_1 = 0.54$ the difference was 176–180%,

for $k_2 = 0.41$ – 203–208% and for $k_3 = 0.32$ – 236–284%). In the case of steel samples, the highest force values occurred for X5CrNi18-10 steel and the lowest for S235JRG2 steel. For $k_1 = 0.54$ the increase was 76–78%, for $k_2 = 0.41$ – 88–159% and for $k_3 = 0.32$ – 97–174%. Apart from differences in the maximum force values, the nature of their changes is very similar regardless of the type of material.

Figures 17 and 18 present exemplary comparisons for S235JRG2 steel and X5CrNi18-10 steel, respectively, determining the influence of collar drawing coefficients on changes in forces with the same punch shapes. With the increase in the degree of material deformation (decrease in the collar drawing coefficient), the values of flanging forces increased with the same punch shapes.

For S235JRG2 steel (Fig. 17), when flanging with a flat punch, the increase in force followed

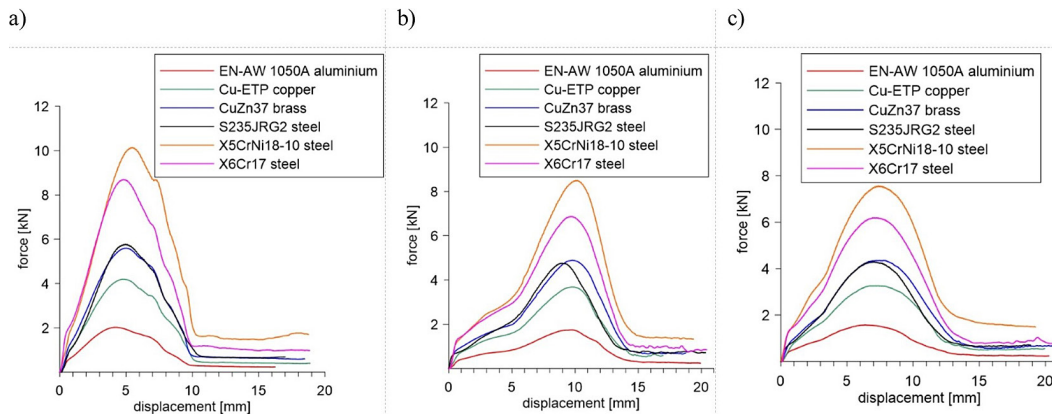


Figure 14. The force vs. displacement obtained for flanging tests from samples made from different materials and the same collar drawing factors $k_1 = 0.54$: a) with flat shape of punch, b) with conical shape of punch, c) with spherical shape of punch

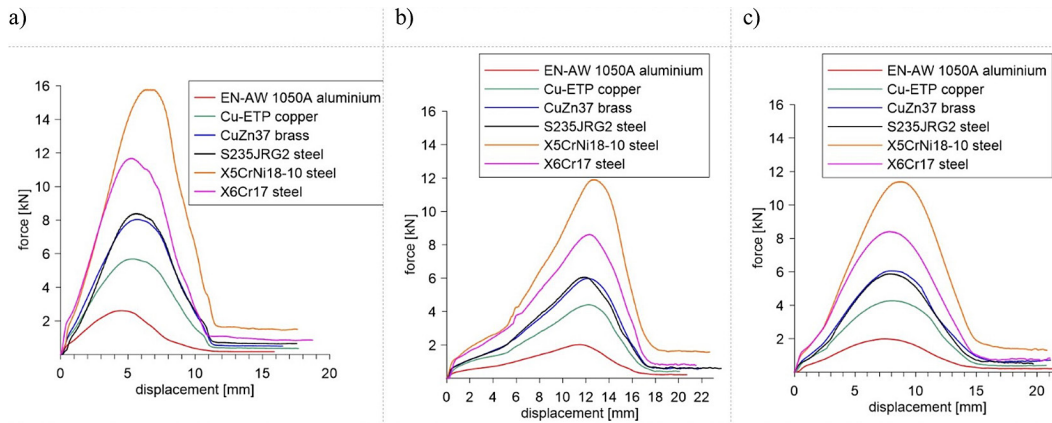


Figure 15. The force vs. displacement obtained for flanging tests from samples made from different materials and the same collar drawing factors $k_1 = 0.41$: a) with flat shape of punch, b) with conical shape of punch, c) with spherical shape of punch

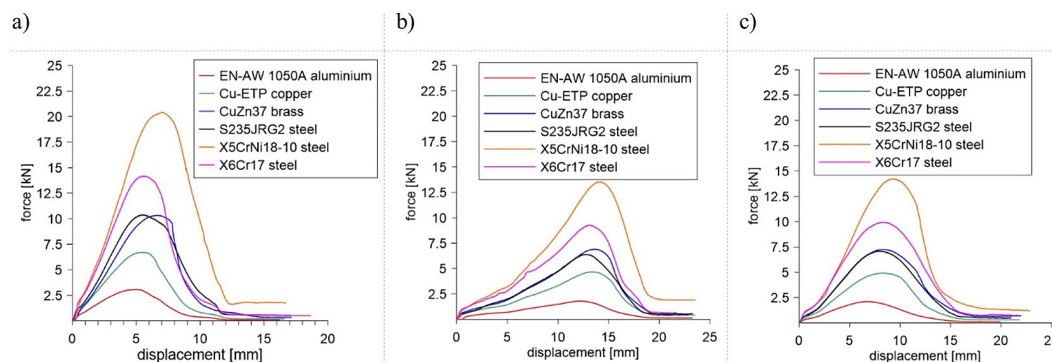


Figure 16. The force vs. displacement obtained for flanging tests from samples made from different materials and the same collar drawing factors $k_1 = 0.32$: a) with flat shape of punch, b) with conical shape of punch, c) with spherical shape of punch

a decrease in the flanging coefficient (from $k_1 = 0.54$ to $k_2 = 0.41$ and $k_3 = 0.32$) by 45% and 80%, respectively. When using a conical punch, it was an increase of 27% and 34%. However, when

using a spherical punch, this increase was 37% and 65%, respectively.

For steel X5CrNi18-10 (Figure 18), the increase in force during flanging occurred with a

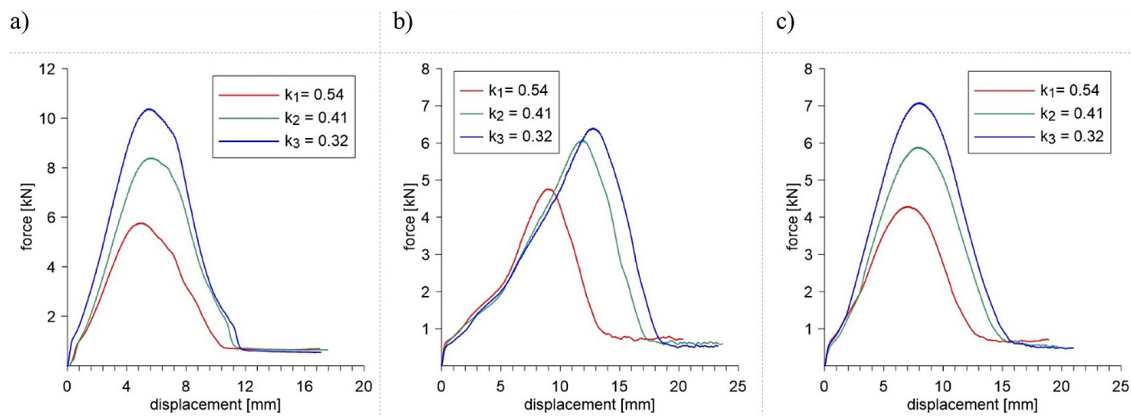


Figure 17. The force vs. displacement obtained for flanging tests from samples made from S235JRG2 steel and different collar drawing factors: a) with flat shape of punch, b) with conical shape of punch, c) with spherical shape of punch

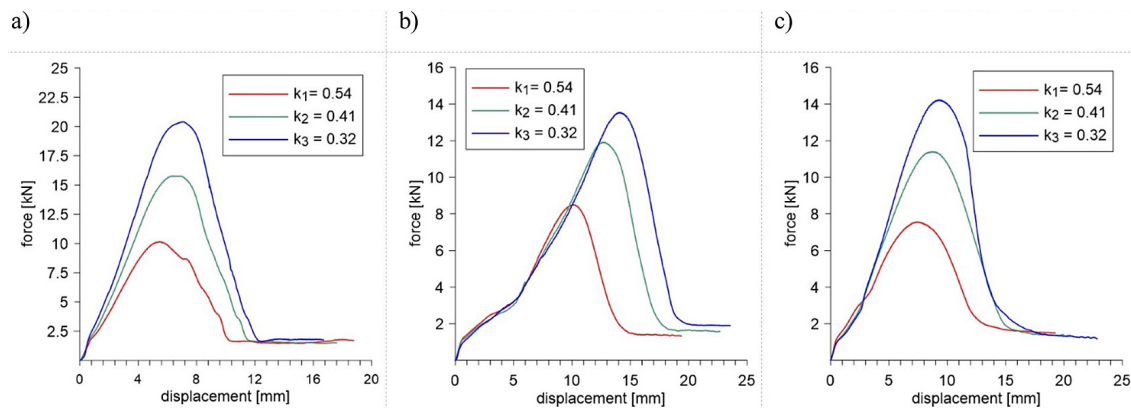


Figure 18. The force vs. displacement obtained for flanging tests from samples made from X5CrNi18-10 steel and different collar drawing factors: a) with flat shape of punch, b) with conical shape of punch, c) with spherical shape of punch

decrease in the collar drawing coefficient by 56% and 101% at a flat punch, by 40% and 59% at a conical punch, and at a spherical punch, this increase was 51% and 88%, respectively.

In both cases (Figures 17 and 18), the force changes for the flat and spherical punches had similar total displacements and displacement values at which the maximum forces occurred, regardless of the different values of the collar drawing coefficients. However, in the case of a conical punch, with the increase in the degree of deformation, the displacement of the punch during flanging increased (for the coefficient of 0.32 in relation to the coefficient of 0.54 by approximately 100%). This can be explained by the fact that with the highest coefficient of collar drawing ($k_1 = 0.54$), the largest hole in the blank was $d = 10$ mm, which allows the conical punch to enter the material deeper than with the hole $d = 6$ mm

for the coefficient $k_3 = 0.32$. In the last stage of the research, the geometric parameters of the flanged edges of the draw pieces were measured. Table 3 shows the average results of measurements of wall thickness g , height of the flanged rim H and external diameters d_f for different materials, shapes of punches and collar drawing coefficients.

Comparing the edge heights obtained during the experiments, it can be seen that regardless of the type of material, for the same collar drawing coefficients, the shapes of the punches used had no significant impact on the obtained height H (differences do not exceed 6%). As the degree of deformation increased, in most cases the thinning of the wall at the edge of the rim g increased (denotation according to Figure 4). For example, in the case of S235JRG2 steel, when flanged with a conical punch for the coefficient $k_1 = 0.54$, the thinning was about

6%, for $k_2 = 0.41$ it was about 16% and for $k_3 = 0.32$ – about 20%.

Figure 19 shows the influence of the total percentage strain on the flange height for different shape of punch and samples made from

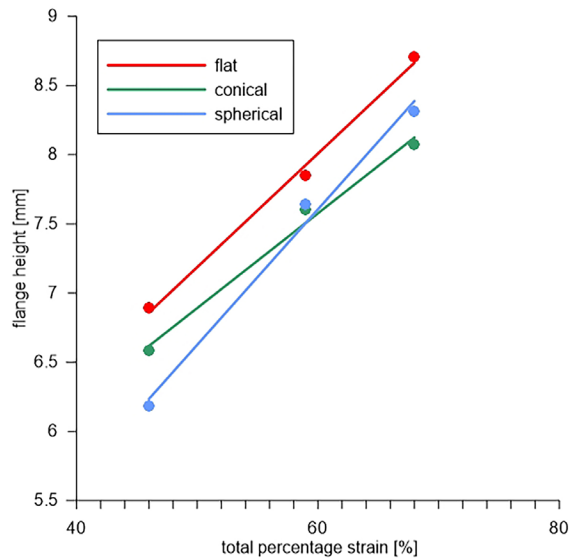


Figure 19. The influence of the total percentage strain on the flange height for different shape of punch and samples made from S235JRG2

S235JRG2. Total percentage strain was calculated according formula [2, 3]:

$$\varepsilon_c = (1 - k) \cdot 100\% \quad (4)$$

where: ε_c – total percentage strain; k – collar drawing factor.

As the degree of deformation (the total percentage strain) increases, the height of the rims increases (Fig. 19). The increase for steel samples is 26% for the flat punch, 23% for the conical punch and 28% for the spherical punch.

No significant influence of the punch shape on the enlargement of the hole d_f during flanging was observed (Table 3). Therefore, it is difficult to agree with the conclusions of the authors [12], who found in their research that the largest enlargement of holes occurs with a conical punch and the smallest with a flat punch.

CONCLUSIONS

From the research carried out on the technological parameters of the process of turning the edges of holes from various types of materials and with various punch shapes, the following conclusions can be drawn:

Table 3. Geometrical parameters (mm) of flanges obtained in investigations

Material	k	Shape of the punch								
		Flat			Conical			Hemispherical		
		H	g	d_f	H	g	d_f	H	g	d_f
EN-AW 1050A	0.54	6.92	0.82	19.39	6.68	0.78	19.48	6.54	0.92	19.25
	0.41	Cracking			Cracking			7.69	0.73	19.05
	0.32	Cracking			Cracking			Cracking		
Cu-ETP	0.54	7.01	0.98	19.63	6.69	0.87	19.41	6.67	0.90	19.28
	0.41	7.95	0.78	19.09	7.86	0.73	19.09	Cracking		
	0.32	Cracking			Cracking			Cracking		
CuZn37	0.54	6.93	0.88	19.39	6.56	0.90	19.21	6.60	0.86	19.18
	0.41	8.01	0.71	19.17	7.69	0.73	19.16	Cracking		
	0.32	Cracking			Cracking			Cracking		
S235JRG2	0.54	6.89	0.82	19.42	6.58	0.91	19.59	6.18	0.87	19.40
	0.41	7.85	0.82	19.24	7.60	0.82	19.37	7.64	0.73	19.19
	0.32	8.71	0.74	19.13	8.07	0.78	19.27	8.31	0.73	19.02
X5CrNi18-10	0.54	6.84	0.84	19.36	6.53	0.88	19.32	6.27	0.93	19.21
	0.41	8.07	0.75	19.17	7.67	0.79	19.11	0.77	0.74	19.25
	0.32	9.11	0.68	19.07	8.14	0.77	19.05	Cracking		
X6Cr17	0.54	6.80	0.84	19.39	6.65	0.92	19.30	6.69	0.93	19.25
	0.41	7.88	0.74	19.12	7.76	0.80	19.26	7.86	0.78	19.30
	0.32	Cracking			Cracking			Cracking		

1. The determined limit collar drawing coefficients for the tested materials are:
 - aluminium $k_1 = 0.54$ at all punch shapes and $k_2 = 0.41$ at a spherical punch,
 - copper and brass $k_1 = 0.54$ at a spherical punch and $k_2 = 0.41$ at flat and conical punches,
 - S235JRG2 steel $k_3 = 0.32$ at all punch shapes,
 - X5CrNi18-10 steel $k_2 = 0.41$ for a spherical punch and $k_3 = 0.32$ for flat and conical punches,
 - X6Cr17 steel $k_2 = 0.41$ at all punch shapes.
2. The flanging force depends on the shape of the punches. For the coefficients $k_1 = 0.54$ and $k_2 = 0.41$, the greatest values of flanging forces for all tested materials were obtained for flat punches, then smaller ones for conical and spherical punches. With the coefficient $k_3 = 0.32$, the highest forces were also obtained for flat punches, but lower for spherical and conical punches respectively.
3. Changes in forces as a function of punch displacement are of a similar nature regardless of the adopted punch shapes, collar drawing coefficients and type of material. At the same coefficients, the graphs differ in the values of the total displacements of the punch during flanging, the maximum force values and the displacement values at which these maximum forces occur. The smallest total displacements occur when flanging with a flat punch, while the largest with a conical punch, regardless of the type of material (an increase of approximately 33–63% depending on the flanging coefficient).
4. The best flanging results were obtained for S235JRG2 and X5CrNi18-10 steel (the highest degrees of deformation and the highest edge heights). Attempts to flange aluminium rims were unsuccessful due to rim cracking, already with the coefficient $k_2 = 0.41$ with flat and conical punches, because the plastic properties are low. To obtain the possibility of collar drawing at this factor, a spherical punch must be used.
5. The shape of the punch when flanging the edges of holes does not significantly affect the thinning of the wall and the height of the edge. As the degree of deformation increased (reducing the collar drawing coefficient), the height of the rims increased, but the thinning of the wall at the edge of the rim also increased.

REFERENCES

1. Pacanowski J. Design of deep drawing process of axisymmetric draw pieces and design press-forming dies T1 Methods and directives for deep drawing of axisymmetric draw pieces (Kielce: Kielce University of Technology), chapter 2018, 125–138 (in Polish)
2. Lange K. 1985 Handbook of metal forming. McGraw-Hill Book Company, chapter 22, 22.1–22.10.
3. Klocke, F. Manufacturing Processes 4 (Berlin Heidelberg: RWTHedition Springer), chapter Sheet Metal Forming 2013, 293–405.
4. Stachowicz F., Estimation of hole-flange ability for deep drawing steel sheets. Archives of Civil and Mechanical Engineering 2008, 8(2), 167–172.
5. Chałupczak J., Miłek T. The influence of punch shape and grade of material on selected parameters of collar drawing process. Rudy i Metale Nieżelazne 1999, 44(11), 591–594 (in Polish).
6. Marciniak Z. Limit strains in deep drawing process of sheet metals (Warsaw: WNT) chapter 1971, 189–225 (in Polish).
7. Gronostajski Z., Pater Z., Madej L., Gontarz A., Lisiecki L., Łukaszek-Sofek A., Łuksza J., Mróz S., Muskalski Z., Muzykiewicz W., Pietrzyk M., Śliwa R.E. Tomczak, J. Wiewiórowska S., Winiarski G., Zasadziński J., Ziółkiewicz S. Recent development trends in metal forming. Archives of Civil and Mechanical Engineering 2019, 19(3), 898–941.
8. Leu D.-K., Chen T.-C., Huang Y.-M. Influence of punch shapes on the collar-drawing process of sheet steel. Materials processing Technology 1999, 88(1–3), 134–146.
9. Huang Y.M., Chien K.H. Influence of cone semi-angle on the formability limitation of the hole-flanging process. The International Journal of Advanced Manufacturing Technology 2002, 19, 597–606.
10. [Huang Y.M. An elasto-plastic finite element analysis of the sheet metal stretch flanging process. The International Journal of Advanced Manufacturing Technology 2007, 34, 641–648.
11. Frącz W., Stachowicz F., Trzepieciński T. Investigations of thickness distribution in hole expanding of thin steel sheets. Archives of Civil and Mechanical Engineering 2012, 12(3), 279–283.
12. Krawczyk J., Gronostajski Z., Polak S., Jaśkiewicz K., Chorzępa W., Pęczak I. The influence of the punch shape and the cutting method on the limit strain in the hole expansion test. Key Engineering Materials: Trans Tech Publ. 2016, 129–37.
13. Kumar S., Ahmed M., Panthi S.K. Effect of punch profile on deformation behaviour of AA5052 sheet in stretch flanging process. Archives of Civil and Mechanical Engineering 2020, 20(18), 1–18.

14. Wang M., Wang S., Li Z. Multi-step forming punch (MFP) for improving stretch-flangeability of advanced high-strength steel. *The International Journal of Advanced Manufacturing Technology* 2018, 99, 1627–1638.
15. Bambach M., Voswinckel H., Hirt G. A new process design for performing hole-flanging operations by incremental sheet forming. *Procedia Engineering* 2014, 81, 2305–2310.
16. Soussi H., Masmoudi N., Krichen A. Analysis of geometrical parameters and occurrence of defects in the hole-flanging process on thin sheet metal. *Journal of Materials Processing Technology* 2016, 234, 228–242.
17. Masmoudi N., Soussi H., Krichen A. Determination of an adequate geometry of the flanged hole to perform formed threads. *The International Journal of Advanced Manufacturing Technology* 2017, 92, 547–560.
18. Balawender T., Śliwa R.E., Kosidło J. Plastic forming of hole flange rims in titanium sheets using thermal effect of friction. *Obróbka Plastyczna Metali* 2017, 28(4), 251–262.
19. ISO, E., 6892-1. *Metallic materials – Tensile testing – Part 1: Method of test at room temperature*, International Organization for Standardization, 2019.